

An efficient approach to global sensitivity analysis and parameter estimation for line gratings

Nando Farchmin^{a,b}, Martin Hammerschmidt^{c,d}, Philipp-Immanuel Schneider^{c,d}, Matthias Wurm^a, Bernd Bodermann^a, Markus Bär^a, and Sebastian Heidenreich^a

^aPhysikalisch-Technische Bundesanstalt, Braunschweig and Berlin

^bTechnische Universität Berlin, Institute of Mathematics

^cJCMwave GmbH

^dZuse Institute Berlin

ABSTRACT

Scatterometry is a fast, indirect and nondestructive optical method for the quality control in the production of lithography masks. Geometry parameters of line gratings are obtained from diffracted light intensities by solving an inverse problem. To comply with the upcoming need for improved accuracy and precision and thus for the reduction of uncertainties, typically computationally expansive forward models have been used. In this paper we use Bayesian inversion to estimate parameters from scatterometry measurements of a silicon line grating and determine the associated uncertainties. Since the direct application of Bayesian inference using Markov-Chain Monte Carlo methods to physics-based partial differential equation (PDE) model is not feasible due to high computational costs, we use an approximation of the PDE forward model based on a polynomial chaos expansion. The expansion provides not only a surrogate for the PDE forward model, but also Sobol indices for a global sensitivity analysis. Finally, we compare our results for the global sensitivity analysis with the uncertainties of estimated parameters.

Keywords: uncertainty quantification, polynomial chaos, global sensitivity analysis, inverse problem, parameter reconstruction, scatterometry

1. INTRODUCTION

Scatterometry is an optical scattering technique frequently used for the characterization of periodic nanostructures on surfaces in semiconductor industry.¹ In contrast to other techniques like electron microscopy, optical microscopy or atomic force microscopy, scatterometry is a non-destructive and indirect method. In particular, geometry parameters of interest are determined by measuring diffraction patterns and solving an inverse problem. A basic requirement for the success of the estimation of parameters is that the underlying model is sensitive to the parameters of interest. The more sensitive a systems dependence on a certain parameter, the easier is the reconstruction of that parameter. On the other hand, when designing numerical models to simulate experiments, it is often unclear which parameters are necessary for the model, often resulting in a large amount of parameters used for the model even if some of them have little or no influence on the system. For both reasons, a sensitivity analysis is often useful. A sensitivity analysis gives a priori information about the influence of input parameters on the output.

Most often, variance based sensitivity indices are computed by using Monte-Carlo methods, which is computationally demanding.^{2,3} Hence, often only the sensitivities of a few, presumably most important parameters are considered. Here we present an expansion into polynomials that yields an algebraic approach to characterize the global sensitivities for all parameters with less computational cost.⁴

In this paper, we determine the geometry parameters of a photomask that consists of multilayered, periodic, straight absorber lines of two optically different materials. The period of the line structure (pitch) is 50 nm and the geometry parameters of interest are the height of the line h , the width at the middle of the line (critical

E-mail: nando.farchmin@ptb.de

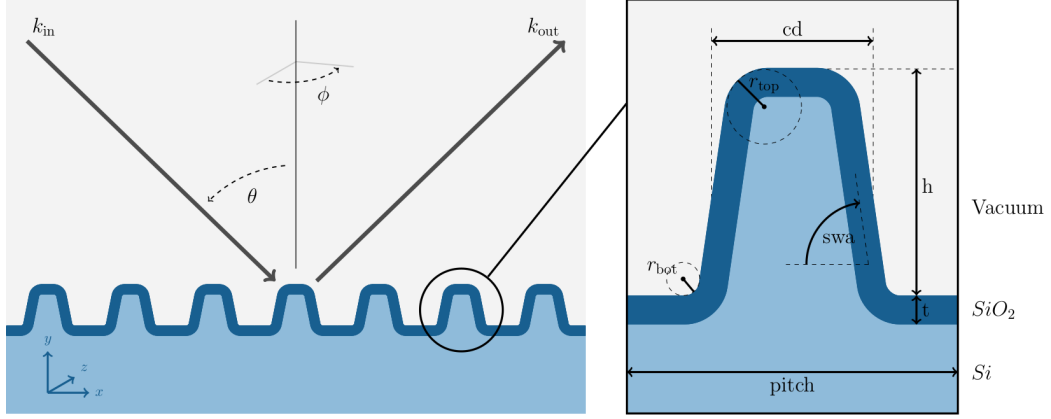


Figure 1. Cross section of the photomask with description of the stochastic parameters. The dimensional parameter vector is given by $\xi = (h, cd, swa, t, r_{top}, r_{bot})$. The pitch, i.e. the length of periodicity is fixed to 50 nm.

dimension) CD, the sidewall angle SWA, the silicon oxide layer thickness t and the radii of the rounding at the top and bottom corners of the line r_{top} and r_{bot} , respectively. A cross section of the geometry for one period of the structure is depicted in Fig. 1. The photomask was illuminated by a light beam of wavelength $\lambda = 266$ nm for different angles of incidence $\theta = 3^\circ, 5^\circ, \dots, 87^\circ$ for perpendicular ($\phi = 0^\circ$) and parallel ($\phi = 90^\circ$) orientation of the beam with respect to the grating structure as well as S and P polarization.

In the next sections, we will proceed as follows. First, we introduce the forward model of the problem, followed by the global sensitivity analysis and Bayesian inversion based on a polynomial chaos expansion. Second, we execute the global sensitivity analysis and estimate the posterior distribution from measurement data. Finally, we compare both results.

2. FORWARD MODEL

In principle, the propagation of electromagnetic waves is described by Maxwell's equations, but for our simple grating geometry Maxwell's equations reduce to a single second order partial differential equation,⁵

$$\nabla \times \mu^{-1} \nabla \times E + \omega^2 \varepsilon E = 0. \quad (1)$$

Here, ε and μ are the permittivity and permeability and ω is the frequency of the incoming beam. The boundary conditions are chosen to be transparent in horizontal and periodic in lateral direction. The resulting boundary value problem is solved by a finite element method (FEM). For computations we used the JCMSuite * software package.

The forward model is given by a map of geometry parameters onto S and P polarization of first order intensities of the scattered light. The parameters ξ used for modelling the grating geometry are depicted in Fig. 1. The forward model is represented by the function $f^*: \Omega \rightarrow \mathbb{R}^d$ such that the parameters $\xi \in \Omega \subset \mathbb{R}^M$ are mapped to diffracted efficiencies for a set of azimuthal angles, incidence angles and polarizations.

To obtain a fast evaluation of the surrogate, the function f^* is expanded into an orthonormal polynomial basis $\{\Phi_\alpha\}_{\alpha \in \Lambda} \subset L^2(\Omega; \varrho)$ ⁶⁻⁸

$$f^*(\xi) \approx f(\xi) = \sum_{\alpha \in \Lambda} f_\alpha \Phi_\alpha(\xi) \quad \text{with} \quad f_\alpha = \int_{\Omega} f(\xi) \Phi_\alpha(\xi) d\varrho(\xi). \quad (2)$$

The finite set $\Lambda \subset \mathbb{N}_0^M$ is a set of multiindices and ϱ denotes the multivariate parameter density for the parameters ξ . With this surrogate the evaluation of the model in different parameter realizations is equivalent to the

*<https://jcmwave.com/jcmsuite>

evaluation of polynomials. Additionally, we remark that this is a nonintrusive method and hence the solver used for the deterministic Helmholtz equation (1) needs no adaptation.⁴

In our approach, the experimental data $y \in \mathbb{R}^d$ are modelled with the error $y_j = f_j(\xi) + \varepsilon_j$, $j = 1, \dots, d$ where $\varepsilon_j \sim \mathcal{N}(0, \sigma_j)$ describes a normal distributed noise with zero mean, standard deviation and error parameter b ,

$$\sigma_j(b) = b y_j, \quad \text{for } b > 0. \quad (3)$$

The inverse problem in scatterometry is defined by the determination of geometry parameter values ξ and the error parameter (hyper parameter) b from measured efficiencies y .

3. GLOBAL SENSITIVITY ANALYSIS

Sensitivity analysis is a broadly used tool to identify the influence of uncertain input parameters upon the output of a physical system or model. Local methods for sensitivity analysis utilize partial derivatives of the output of the system with respect to the various uncertain input parameters to obtain the local parameter dependence of the system.⁹ However, since local sensitivity analysis does not cover the hole input space, only small perturbations can be observed. Global variance-based sensitivity analysis on the other hand decomposes the total system variance $\text{Var}[f^*]$ over the complete parameter space into parts attributing to input parameters and combinations thereof.^{10,11} Among the vast collection of variance-based methods for sensitivity analyses, Sobol indices are a common and widely spread method to characterize parameter sensitivities. The map f^* from above with expectation $\mathbb{E}[f^*]$ and variance $\text{Var}[f^*]$ can be decomposed as¹⁰

$$f^*(\xi) = S_0 + \sum_{1 \leq s \leq M} \sum_{j_1 < \dots < j_s \in \mathcal{M}} S_{j_1, \dots, j_s}(\xi_{j_1}, \dots, \xi_{j_s}) \quad \text{for } \mathcal{M} = \{1, \dots, M\}, \quad (4)$$

into functions S_{j_1, \dots, j_s} depending exactly on the parameters $\xi_{j_1}, \dots, \xi_{j_s}$. Inserting this decomposition into the computation of the variance of the map f^* then yields the Sobol indices, i.e.

$$\text{Sob}_{j_1, \dots, j_s} = \frac{\text{Var}[S_{j_1, \dots, j_s}]}{\text{Var}[f^*]}. \quad (5)$$

Computing the variances in the equation above requires high dimensional integration. These integration is often calculated by Monte-Carlo methods that require many expensive function evaluations.

It was previously shown,⁴ that the uniqueness of the PC expansion and the uniqueness of the Sobol decomposition (4), gives the algebraic equivalence

$$\text{Sob}_{j_1, \dots, j_s} \approx \frac{\sum_{\alpha \in \Lambda_{j_1, \dots, j_s}} f_\alpha^2}{\sum_{\alpha \in \Lambda \setminus \{0\}} f_\alpha^2}. \quad (6)$$

Here $\Lambda_{j_1, \dots, j_s} \subset \Lambda$ is the set of multiindices that differ from zero in exactly the components j_1, \dots, j_s . Note, that the " \approx " in (6) is a result of truncating to finitely many terms in the PC expansion. If the complete PC expansion is used, equality holds in (6).

4. BAYESIAN APPROACH

The Bayesian approach provides a statistical method to solve the inverse problem. Following Bayes' theorem, the posterior density is given by

$$\pi(\hat{\xi}; y) = \frac{\mathcal{L}(\hat{\xi}; y) \pi_0(\hat{\xi})}{\int \mathcal{L}(\hat{\xi}; y) \pi_0(\hat{\xi}) d\hat{\xi}}, \quad (7)$$

where the prior density π_0 describes prior knowledge and the likelihood function \mathcal{L} contains the information obtained from the measurement. The vector $\hat{\xi}$ consists of geometry parameters ξ and the noise parameter, i.e. $\hat{\xi} = (\xi, b)$. Assuming normal distributed measurement errors, we choose the likelihood function¹²

$$\mathcal{L}(\hat{\xi}; y) = \prod_{j=1}^d \frac{1}{\sqrt{2\pi}\sigma_j(b)} \exp\left(-\frac{(f_j(\xi) - y_j)^2}{2\sigma_j^2(b)}\right). \quad (8)$$

In the Bayesian framework, the distributions of parameters are in general determined by Markov Chain Monte Carlo (MCMC) sampling where for every sampling step, the forward model has to be evaluated. Normally, this means that the Helmholtz equation has to be solved which makes MCMC sampling impractical due to the large number of required sampling steps. Since the surrogate only requires evaluations of polynomials, the Bayesian approach becomes practical for scatterometry measurement evaluations.¹³

Table 1. Estimations of parameters and uncertainties obtained from the mean value (mean), the standard deviation (std) and relative standard deviation (rel.std) of the posterior distribution. The domain indicates the support of the prior distribution chosen.

parameter	domain	mean	std	rel.std
h	[43.0, 53.0] nm	48.35 nm	1.56 nm	0.3112
cd	[22.0, 28.0] nm	25.48 nm	0.30 nm	0.099
swa	[84.0, 90.0]°	86.87°	1.33°	0.4424
t	[4.0, 6.0] nm	4.96 nm	0.18 nm	0.1756
r_{top}	[8.0, 13.0] nm	10.65 nm	1.15 nm	0.4601
r_{bot}	[3.0, 7.0] nm	4.89 nm	0.90 nm	0.4495
b	[0.0, 0.1]	0.01	0.0021	0.0849

For Bayesian inversion, we have to choose a prior distribution for the parameters, calculate the likelihood function and determine the corresponding posterior distribution. The posterior distribution contains the desired parameter values and their associated uncertainties. When two or more measurement results from different measurement sets $y^{(1)}, \dots, y^{(K)}$ are combined, the posterior distribution of the first measurement can be used as the prior distribution for the evaluation of the second measurement, i.e.

$$\pi(\hat{\xi}; y^{(K)}, y^{(K-1)}, \dots, y^{(1)}) = \frac{\pi_0(\hat{\xi}) \prod_{k=1}^K \mathcal{L}(\hat{\xi}; y^{(k)})}{\int \pi_0(\hat{\xi}) \prod_{k=1}^K \mathcal{L}(\hat{\xi}; y^{(k)}) d\hat{\xi}}. \quad (9)$$

Note that the model function f in the likelihood function is in general different for different measurement setups.

5. RESULTS

For the geometry presented above, we calculated the Sobol indices Eq.(5) for all parameters as depicted in Fig. 2. Boxplots for perpendicular and parallel beam incidence as well as S and P polarization are shown, respectively, over 43 angles of incidence θ . The sensitivity parameter correlation is very small and is therefore omitted here. First of all, we note that the height, critical dimension and oxide layer thickness make up most of the total variance. The sensitivity depends also on the polarization and the angle of incidence. For example, the oxide layer thickness t is most sensitive with respect to the S polarization for a perpendicular beam orientation ($\phi = 0^\circ$) and the sidewall angle depends highly on the angle of incidence (P polarization, parallel to the beam).

With this, we expect that the reconstruction of all parameters is feasible. In particular, the oxide layer thickness and critical dimension should be possible to determine precisely due to their high sensitivity.

Next, we apply Bayesian inversion on scatterometry measurements to estimate geometry parameters of the line grating. More details of the measurement setup are described in.^{5,14} For Bayesian inversion it is necessary

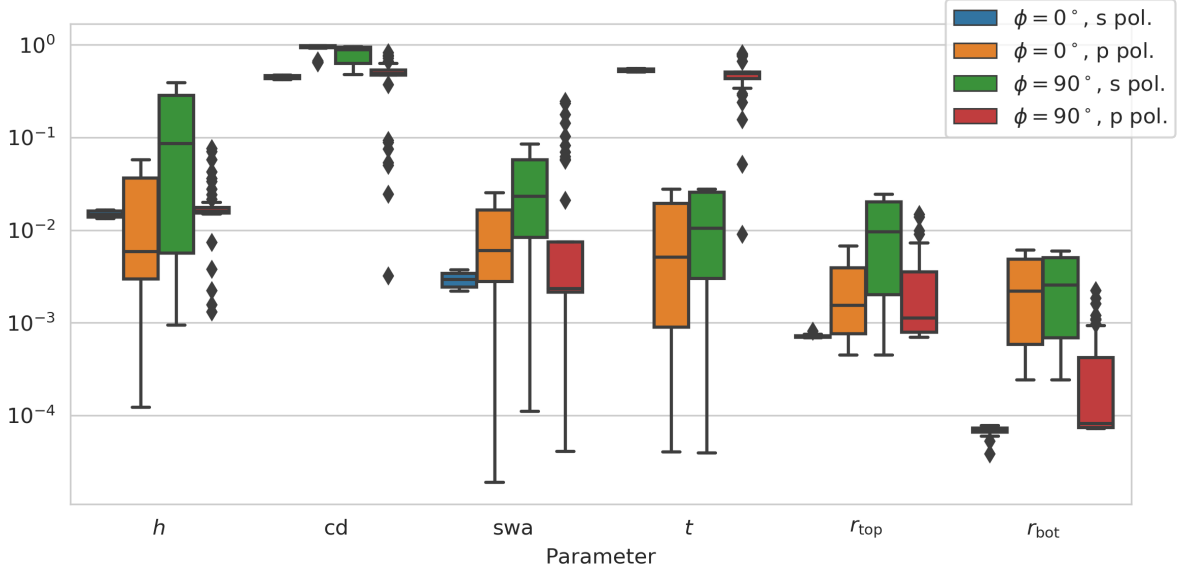


Figure 2. Boxplots of Sobol indices for all geometry parameters, azimuthal angles and polarization. Each boxplot includes Sobol indices for the whole range of angles of incidence.

to chose prior distributions. In our investigations we have chosen uniform priors on the domains given in Table 1. To obtain the posterior distribution, we sampled with a MCMC random walk Metropolis algorithm using the surrogate. We have chosen a sampling size of 10^6 samples and a burn in phase of 10^4 samples. For diagnostics, we applied the Gelman-Rubin criterion,¹⁵ to assure that generated samples are independent. We calculated the marginal posterior densities for all 6 stochastic parameters. All posterior densities are characterized by sharp peaks with mean and standard deviation similar to the previous publication.⁵ The mean and standard deviation for each parameter including the hyperparameter (error parameter) b are shown in Table 1. Since the domain sizes of the parameters vary due to their geometrical meaning, we introduce the relative standard derivation (std). The relative std is the std divided by half the width of the parameter domain:

$$\text{rel.std}(\eta) = \frac{2 \text{std}(\eta)}{\beta - \alpha} \quad \text{where } \eta \in [\alpha, \beta]. \quad (10)$$

The relative std shows how the posterior distribution is spread within the domain. For example, if the domain for the critical dimension is $[22, 28]$ nm, and the std is 0.3 nm then the relative std is $\text{rel.std} = 0.099$, i.e. the posterior distribution is concentrated in about 10% of the original domain. This way we can deduce how wide the parameter distributions are spread across the reconstruction domains. The relative std in Table 1 shows that the smallest reconstruction uncertainties are obtained for the critical dimension with relative std about 10%, followed by the oxide layer thickness with 18% relative std. The height has a relative std of about 31%. The posterior densities of the sidewall angle and the corner rounding are slightly wider distributed at about 45% relative std. This goes in line with the global sensitivity analysis (see Fig. 2).

The results for the error parameter b depicted in Table 1 show that the relative measurement uncertainty is approximately 1%.

Finally, Fig. 3 displays a comparison between the measurement data and the evaluation of our surrogate model using reconstructed geometry parameters. The pointwise relative deviation of the approximation from the measurements data is 2% and lower. In⁵ the measurement data were evaluated by a Maximum Posterior Approach (MPA). The MPA searches the global maximum of the posterior and uncertainties are determined by the local covariance matrix. The difference here is that we calculated the whole posterior distribution. This has the advantage that even for multiple peaked and non-Gaussian posterior distributions this scheme gives reliable uncertainty estimations. The results obtained in⁵ are consistent to our findings. There are only slight differences. For example, the marginal distribution for the height h is broad (non-Gaussian) yielding larger

uncertainties. Similarly, the mean values for r_{top} and r_{bottom} are slightly shifted due to the asymmetry of the marginal posterior (non-Gaussian). The deviation between the forward model values and the measurement data of 2% is comparable with that found in.⁵

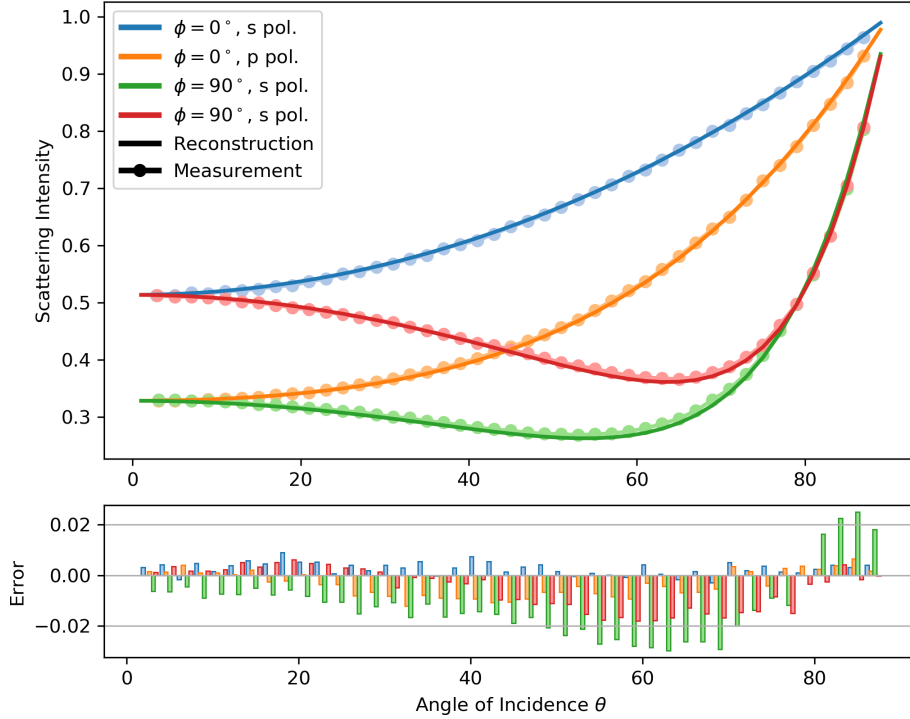


Figure 3. Scattered intensities for the two polarizations and different azimuthal angles. Compared are the measurements of the scatterometry experiment and the simulation of the PC surrogate for the mean values of the parameter reconstruction. The bottom graph shows the pointwise deviation.

6. SUMMARY

In this paper we applied a polynomial chaos expansion as a surrogate for the forward model in scatterometry. This approach enables us to perform a global sensitivity analysis at low computational costs. Moreover, since the surrogate only requires the evaluation of polynomials instead of solving the Helmholtz equation, it was feasible to use a full Bayesian approach to determine the posterior distribution for all geometry parameters. To generate samples from the posterior distribution, we employed a MCMC Metropolis random walk sampling method and checked the overall independence of the samples obtained by the Gelman-Rubin criterion. The reconstruction results obtained by the surrogate model compared to those obtained by a Maximum Posterior estimate with a Gauss-Newton like method⁵ are consistent and are in line with the predictions from our global sensitivity analysis. We finally conclude that a Bayesian approach based on the polynomial chaos surrogate gives accurate and reliable estimations for silicon line grating parameters and uncertainties.

REFERENCES

- [1] Hsu, S. and Terry, F., “Spectroscopic ellipsometry and reflectometry from gratings (scatterometry) for critical dimension measurement and in situ, real-time process monitoring,” *Thin Solid Films* **455**, 828–836 (2004).
- [2] Homma, T. and Saltelli, A., “Importance measures in global sensitivity analysis of nonlinear models,” *Reliability Engineering and System Safety* **52**(1), 1–17 (1996).

- [3] Saltelli, A., Annoni, P., Azzini, I., Campolongo, F., Ratto, M., and Tarantola, S., “Variance based sensitivity analysis of model output. design and estimator for the total sensitivity index,” *Computer Physics Communications* **181**(2), 259 – 270 (2010).
- [4] Sudret, B., “Global sensitivity analysis using polynomial chaos expansions,” *Reliability Engineering and System Safety* **93**(7), 964–979 (2008).
- [5] Hammerschmidt, M., Weiser, M., Santiago, G. X., Zschiedrich, L., Bodermann, B., and Burger, S., “Quantifying parameter uncertainties in optical scatterometry using bayesian inversion,” *Proc. SPIE 10330, Modeling Aspects in Optical Metrology* (2017).
- [6] Wiener, N., “The Homogeneous Chaos,” *Amer. J. Math.* **60**(4), 897–936 (1938).
- [7] Cameron, R. H. and Martin, W. T., “The orthogonal development of non-linear functionals in series of Fourier-Hermite functionals,” *Ann. of Math. (2)* **48**, 385–392 (1947).
- [8] Ghanem, R. and Spanos, P.-T., “Polynomial chaos in stochastic finite elements,” *Journal of Applied Mechanics-Transactions of The Asme - J APPL MECH* **57**, 197–202 (03 1990).
- [9] Saltelli, A. and Annoni, P., “How to avoid a perfunctory sensitivity analysis,” *Environmental Modelling and Software* **25**(12), 1508 – 1517 (2010).
- [10] Sobol, I. M., “Sensitivity estimates for nonlinear mathematical models,” *Math. Modeling Comput. Experiment* **1**(4), 407–414 (1995) (1993).
- [11] Sobol, I. M., “Global sensitivity indices for nonlinear mathematical models and their Monte Carlo estimates,” *Math. Comput. Simulation* **55**(1-3), 271–280 (2001).
- [12] Heidenreich, S., Gross, H., and Bar, M., “Bayesian approach to the statistical inverse problem of scatterometry: Comparison of three surrogate models,” *International Journal for Uncertainty Quantification* **5**(6) (2015).
- [13] Heidenreich, S., Gross, H., and Bär, M., “Bayesian approach to determine critical dimensions from scatterometric measurements,” *Metrologia* **55**(6), S201 (2018).
- [14] Wurm, M., Bonifer, S., Bodermann, B., and Richter, J., “Deep ultraviolet scatterometer for dimensional characterization of nanostructures: system improvements and test measurements,” *Measurement Science and Technology* **22**(9), 094024 (2011).
- [15] Gelman, A. and Rubin, D. B., “Inference from iterative simulation using multiple sequences,” *Statistical Science* **7**(4), 457–472 (1992).
- [16] Agocs, E., Bodermann, B., Burger, S., Dai, G., Endres, J., Hansen, P.-E., Nielson, L., Madsen, M. H., Heidenreich, S., Krumrey, M., et al., “Scatterometry reference standards to improve tool matching and traceability in lithographical nanomanufacturing,” in [*Nanoengineering: Fabrication, Properties, Optics, and Devices XII*], **9556**, 955610, International Society for Optics and Photonics (2015).
- [17] Heidenreich, S., Gross, H., Henn, M., Elster, C., and Bär, M., “A surrogate model enables a bayesian approach to the inverse problem of scatterometry,” in [*Journal of Physics: Conference Series*], **490**(1), 012007, IOP Publishing (2014).
- [18] Heidenreich, S., Gross, H., Wurm, M., Bodermann, B., and Bär, M., “The statistical inverse problem of scatterometry: Bayesian inference and the effect of different priors,” in [*Modeling Aspects in Optical Metrology V*], **9526**, 95260U, International Society for Optics and Photonics (2015).